

# Photocatalytic Reduction of Carbon Dioxide to CO and HCO<sub>2</sub>H Using *fac*-Mn(CN)(bpy)(CO)<sub>3</sub>

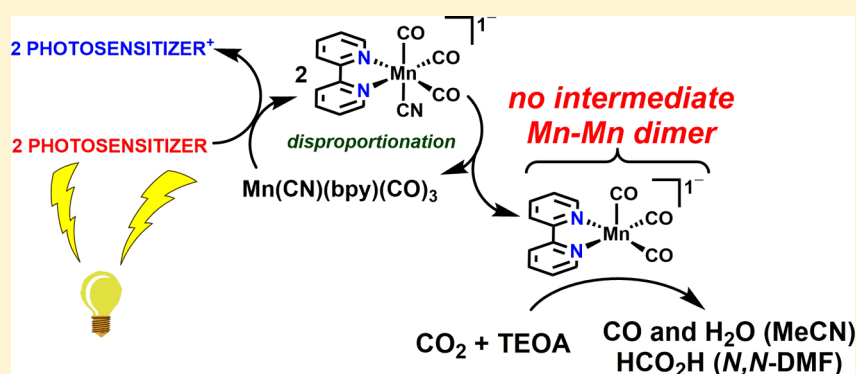
Po Ling Cheung,<sup>†</sup> Charles W. Machan,<sup>†</sup> Aramice Y. S. Malkhasian,<sup>‡</sup> Jay Agarwal,<sup>§</sup> and Clifford P. Kubiak<sup>\*,†</sup>

<sup>†</sup>Department of Chemistry and Biochemistry, University of California, San Diego, California 92093, United States

<sup>‡</sup>Chemistry Department, King Abdulaziz University, Jeddah, 21589, Saudi Arabia

<sup>§</sup>Center for Computational Quantum Chemistry, University of Georgia, Athens, Georgia 30602, United States

## S Supporting Information



**ABSTRACT:** Studies are reported regarding the use of  $\text{Mn}(\text{CN})(\text{bpy})(\text{CO})_3$  (**1**) as a catalyst for  $\text{CO}_2$  reduction employing  $[\text{Ru}(\text{dmb})_3]^{2+}$  as a photosensitizer in mixtures of dry *N,N*-dimethylformamide-triethanolamine (*N,N*-DMF-TEOA) or acetonitrile-TEOA (MeCN-TEOA) with 1-benzyl-1,4-dihydropyridine as a sacrificial reductant. Irradiation with 470 nm light for up to 15 h yields both CO and HCO<sub>2</sub>H with maximum turnover numbers (TONs) as high as 21 and 127, respectively, with product preference dependent on the solvent. Further data suggests that upon single electron reduction this catalyst avoids the formation of a Mn–Mn dimer and instead undergoes a disproportionation reaction, which requires 2 equiv of  $[\text{Mn}(\text{CN})(\text{bpy})(\text{CO})_3]^{*-}$  to generate 1 equiv each of the active catalyst  $[\text{Mn}(\text{bpy})(\text{CO})_3]^-$  and the starting compound **1**. Additional characterization by cyclic voltammetry (CV) and infrared spectroelectrochemistry (IR-SEC) indicates that the stability of the singly reduced  $[\text{Mn}(\text{CN})(\text{bpy})(\text{CO})_3]^{*-}$  differs slightly in the *N,N*-DMF-TEOA solvent system compared to the MeCN-TEOA system. This contributes to the observed selectivities for HCO<sub>2</sub>H vs CO production.

## INTRODUCTION

Global warming from anthropogenic greenhouse gas emissions and the decreasing availability of fossil fuels continues to highlight the potential for photocatalytic conversion of carbon dioxide ( $\text{CO}_2$ ) to generate chemicals or fuel precursors, such as synthesis gas ( $\text{CO}/\text{H}_2$ ). These products can be converted into liquid fuels through the industrial Fischer–Tropsch reaction.<sup>1–3</sup> Therefore, the development of artificial photosynthetic systems to harness renewable energy for this purpose is consequently important. Molecular catalysts with Ru- and Re-carbonyl cores and ligands based on 2,2′-bipyridine (bpy) have been investigated extensively for their photocatalytic performance in this context.<sup>4–9</sup> Complexes of this type have been used to convert  $\text{CO}_2$  to carbon monoxide (CO) and/or formic acid (HCO<sub>2</sub>H) using a photosensitizer to initiate photochemical electron transfer along with a sacrificial reductant to donate electrons and sustain catalysis. However, the cost of Ru and Re precludes their use on a large scale, underscoring the need for earth-abundant alternatives, e.g., Mn.<sup>10,11</sup> Although it is not the

focus of the present work, we note that there is a complementary focus on the development of photosensitizers that do not use heavy metals for similar reasons.<sup>12–14</sup>

Prior reports have focused on the electrochemical<sup>15</sup> and photosensitizer-driven<sup>16,17</sup> reactions of *fac*-MnBr(bpy)(CO)<sub>3</sub> (the *fac* label will be omitted from here on). During electrocatalysis, MnBr(bpy)(CO)<sub>3</sub> is first reduced by a single electron, after which the Br<sup>−</sup> ligand dissociates and a metal–metal bonded dimer,  $[\text{Mn}(\text{bpy})(\text{CO})_3]_2$ , is formed.<sup>18,19</sup> Further reduction of the dimer with two electrons yields 2 equiv of the proposed active species,  $[\text{Mn}(\text{bpy})(\text{CO})_3]^-$ ; this reduced species can react with  $\text{CO}_2$  in the presence of added Brønsted acids to produce CO in nonaqueous media.<sup>18,20,21</sup> The intermediate steps are proposed to involve a hydroxycarbonyl species,  $[\text{Mn}(\eta^1\text{-COOH})(\text{bpy})(\text{CO})_3]$ , which forms from the initial reaction of the  $[\text{Mn}(\text{bpy})(\text{CO})_3]^-$  anion with  $\text{CO}_2/\text{H}^+$

Received: February 15, 2016

Table 1. Summary of Catalytic Experiments for Photocatalysis<sup>a</sup>

entry	Mn(CN)(bpy)(CO) <sub>3</sub> /mM	[Ru(dmb) <sub>3</sub> ] <sup>2+</sup> /mM	irradiation time/h	HCO <sub>2</sub> H TON	CO TON	H <sub>2</sub> TON	HCO <sub>2</sub> H Φ	CO Φ
Catalytic Experiments in <i>N,N</i> -DMF-TEOA								
1	0.10	0.10	15	36	3.9	0.64	0.0096	0.0010
2	0.50	0.50	15	21	3.2	0.45	0.031	0.0047
3	1.00	1.00	15	9.5	2.3	0.37	0.027	0.0066
4	0.10	0.10	6	16	2.8	0.20	0.011	0.0018
5	0.50	0.50	6	11	0.92	0.25	0.039	0.0033
6	1.00	1.00	6	5.2	0.83	0.0073	0.033	0.0053
Catalytic Experiments in MeCN-TEOA								
7	0.10	0.10	15	4.5	7.9	0.56	0.0011	0.0020
8	0.50	0.50	15	2.1	5.9	0.24	0.0027	0.0069
9	1.00	1.00	15	1.2	3.2	0.17	0.0029	0.0080
10	0.10	0.10	6	0.00	4.7	0.27	0.00	0.0032
11	0.50	0.50	6	0.00	3.4	0.14	0.00	0.011
12	1.00	1.00	6	0.00	3.1	0.14	0.00	0.021
Variable Concentration Studies in <i>N,N</i> -DMF-TEOA								
13	0.10	0.50	15	130	9.1	1.2	0.026	0.0018
14	0.10	1.00	15	130	7.1	1.6	0.032	0.0018
15	1.00	0.50	15	5.8	3.0	0.24	0.014	0.0070
Variable Concentration Studies in MeCN-TEOA								
16	0.10	0.50	15	8.1	19	1.4	0.0021	0.0048
17	0.10	1.00	15	9.0	21	1.3	0.0022	0.0053
18	1.00	0.50	15	1.4	4.2	0.18	0.0032	0.0096

<sup>a</sup>All runs were sparged with CO<sub>2</sub> for 30 min prior irradiation with 470 nm monochromatic light for 15 h.

Table 2. Summary of Control Experiments for Photocatalysis<sup>a</sup>

entry	Mn(CN)(bpy)(CO) <sub>3</sub> /mM	[Ru(dmb) <sub>3</sub> ] <sup>2+</sup> /mM	sparging gas	HCO <sub>2</sub> H TON	CO TON	H <sub>2</sub> TON	HCO <sub>2</sub> H Φ	CO Φ
Control Reactions in <i>N,N</i> -DMF								
19	0.50	0	CO <sub>2</sub>	1.9	2.1	0.00	0.0022	0.0025
20	0	0.50	CO <sub>2</sub>	5.7	1.5	2.8	0.0069	0.0018
21 <sup>b</sup>	0.50	0.50	CO <sub>2</sub>	0.00	5.8	0.26	0.00	0.0082
22 <sup>c</sup>	0.50	0.50	Ar	2.6				
23	0.50	0.50	Ar	3.8	1.5	7.8	0.0047	0.0018
24	0	0.50	Ar	3.2	0.87	1.3	0.0040	0.0011
25	0.50	0	Ar	2.2	2.3	0.00	0.0030	0.0030
26 <sup>b</sup>	0.50	0.50	Ar	0.00	2.4	1.4	0.00	0.0021
Control Reactions in MeCN								
27	0.50	0	CO <sub>2</sub>	0.00	2.0	0.00	0.00	0.0024
28	0	0.50	CO <sub>2</sub>	0.72	0.60	1.2	0.00093	0.00078
29 <sup>b</sup>	0.50	0.50	CO <sub>2</sub>	0.00	2.2	0.00	0.00	0.0025
30	0.50	0.50	Ar	0.55	2.2	4.4	0.00066	0.0026
31 <sup>b</sup>	0.50	0.50	Ar	0.00	2.4	1.4	0.00	0.0021

<sup>a</sup>All runs were irradiated with 470 nm monochromatic light for 15 h. <sup>b</sup>TEOA is not used in the solvent system. <sup>c</sup>Irradiation time = 0 h.

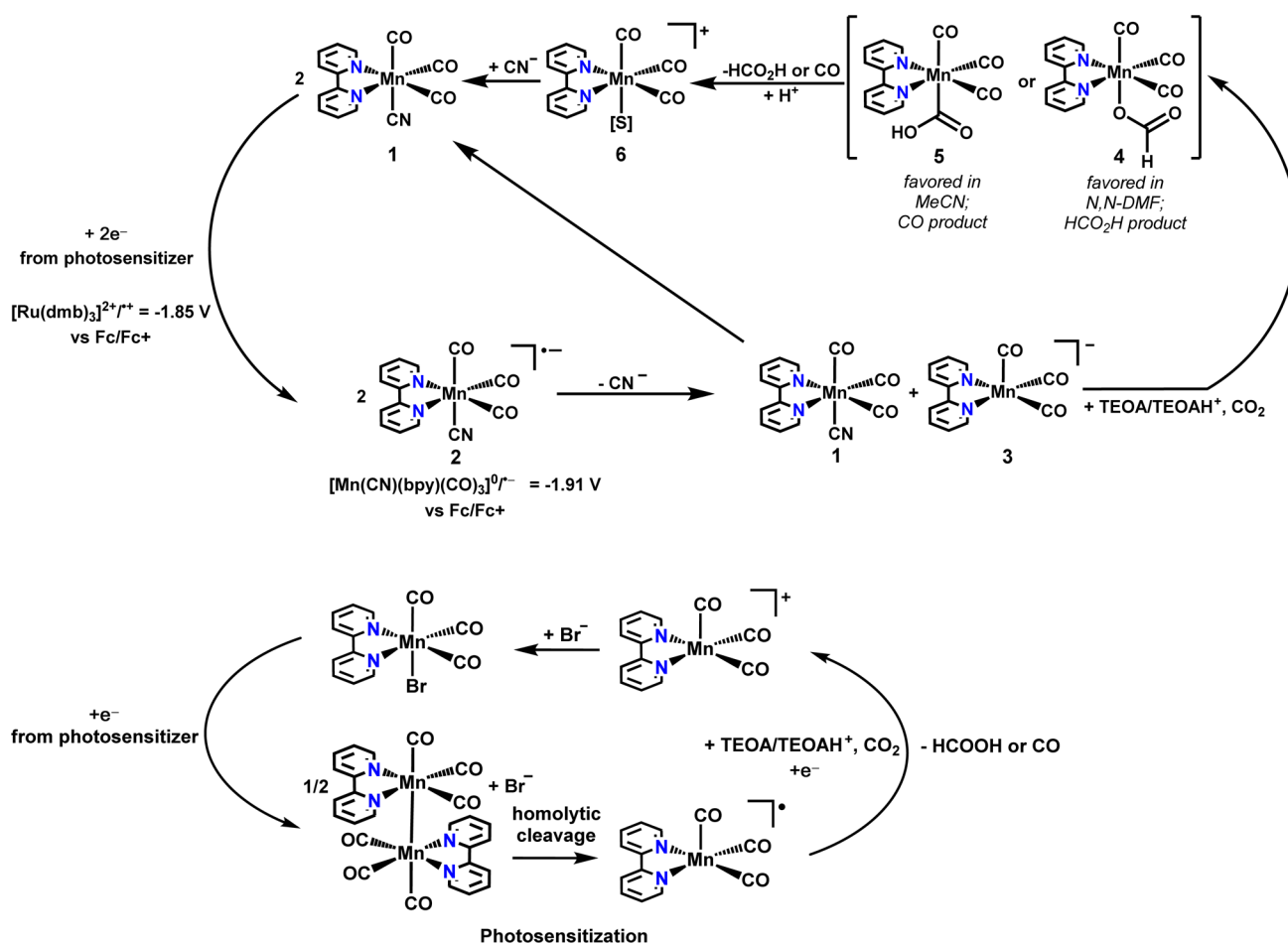
and requires an additional reduction to achieve the highest rate of catalysis.<sup>20,22</sup> Consistent with the electrochemical mechanism detailed above, Takeda et al.<sup>16</sup> found that, as a catalyst, MnBr(bpy)(CO)<sub>3</sub> forms the [Mn(bpy)(CO)<sub>3</sub>]<sub>2</sub> dimer rapidly following a photoinduced one-electron reduction by a photosensitized [Ru(dmb)<sub>3</sub>]<sup>2+</sup> complex. Time-resolved experiments estimate the dimerization rate constant to be rapid, with  $2k_{\text{dim}} = 1.3 \pm 0.1 \times 10^9 \text{ M}^{-1} \text{ s}^{-1}$ .<sup>19</sup> The authors<sup>16</sup> suggested a monomeric, five-coordinate manganese radical species [Mn(bpy)(CO)<sub>3</sub>]<sup>•</sup> results from photoinduced homolytic dimer cleavage; this radical is also proposed to be the active catalyst for reduction of CO<sub>2</sub>, with HCO<sub>2</sub>H as the major product. Analogous Mn radical species have been previously detected as a product of the photoassisted cleavage of Mn–Mn bonds.<sup>23–25</sup>

In a recent report we described the electrocatalytic behavior of Mn(CN)(bpy)(CO)<sub>3</sub> (**1**), which was found to be a

competent catalyst for the electrocatalytic reduction of CO<sub>2</sub> with high Faradaic yield for CO (98 ± 3%).<sup>26</sup> With the substitution of the Br<sup>−</sup> ligand for the pseudohalogen cyanide (CN<sup>−</sup>), the mechanism of catalytic CO<sub>2</sub> reduction was altered from that described above. Specifically, CN<sup>−</sup> did not readily dissociate like Br<sup>−</sup> following a one-electron reduction, mitigating the formation of the Mn–Mn dimer species as an intermediate to the active state, [Mn(bpy)(CO)<sub>3</sub>]<sup>−</sup>, which was instead generated after a disproportionation reaction. As a result, we were interested in investigating the photocatalytic properties of **1** to see if the alternate reduction mechanism would also impact the distribution of two-electron products (H<sub>2</sub>, CO, and HCO<sub>2</sub>H).<sup>16</sup>

Herein, the use of **1** as part of a photocatalytic system for the reduction of CO<sub>2</sub> is reported. The results suggest that, similar to the previously described electrochemical mechanism, **1**

Scheme 1. Proposed Mechanisms for the Formation of HCO<sub>2</sub>H and/or CO from the Photocatalytic Reaction with Mn(CN)(bpy)(CO)<sub>3</sub> (1, top) and MnBr(bpy)(CO)<sub>3</sub><sup>16,17</sup> (bottom)



undergoes a disproportionation reaction involving two singly reduced species,  $[\text{Mn}(\text{CN})(\text{bpy})(\text{CO})_3]^{*\bullet-}$ , to produce 1 equiv of the catalytically active species  $[\text{Mn}(\text{bpy})(\text{CO})_3]^-$  and 1 equiv of 1. Indeed, under a variety of experimental conditions 1 is capable of photocatalytically converting CO<sub>2</sub> to both CO and HCO<sub>2</sub>H, although at lower rates than previously reported for MnBr(bpy)(CO)<sub>3</sub>. Interestingly, the preferred catalytic product shifts from CO to HCO<sub>2</sub>H when changing the solvent from MeCN to N,N-DMF. Supplementary electrochemical and infrared spectroelectrochemical studies support the disproportionation mechanism, and indicate that the N,N-DMF-TEOA mixture is noninnocent with respect to the production of HCO<sub>2</sub>H. This is noteworthy because many studies have focused on the electro- and photocatalytic performance of molecular catalysts related to MnX(bpy)(CO)<sub>3</sub>,<sup>4–9,16,17</sup> but few studies investigate the role of solvent.<sup>8,27,28</sup> Indeed, some reports note that N,N-DMF can be hydrolyzed to produce formate either during photocatalysis or during analysis if significant amounts of water are present.<sup>27,28</sup>

## RESULTS AND DISCUSSION

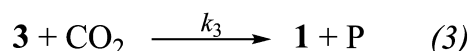
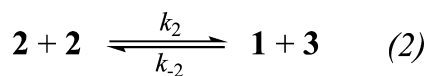
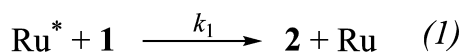
**Photocatalytic Experiments.** Thirty-one photocatalytic experiments with different reaction conditions were conducted, and the results are summarized in Tables 1 and 2. In a typical photocatalytic experiment—adapted from a previous report<sup>17</sup>—a quartz cell of known volume was charged with solvent mixtures of acetonitrile (MeCN) and triethanolamine

(TEOA) (4:1 v/v) or N,N-dimethylformamide (N,N-DMF) and TEOA (4:1 v/v) that contained 1,  $[\text{Ru}(\text{dmb})_3]^{2+}$  as a photosensitizer, and 1-benzyl-1,4-dihydropyridinamide (BNAH, 0.1 M) as a sacrificial reductant. After irradiation at 470 nm with an LED laser, the gaseous products (CO, H<sub>2</sub>) were quantified by GC and liquid products (HCO<sub>2</sub>H) with <sup>1</sup>H NMR (see Experimental Methods). A key finding is that the main product of the photochemical reaction was HCO<sub>2</sub>H in the N,N-DMF-TEOA solvent system, while CO was the primary product in MeCN-TEOA, vide infra.

In the following sections we highlight two conclusions that are supported by these experimental results: (i) complex 1 follows a disproportionation mechanism under photocatalytic conditions and (ii) varying the solvent system from N,N-DMF-TEOA to MeCN-TEOA affects the product distribution between HCO<sub>2</sub>H and CO. We discuss the origin of these conclusions and introduce further experimental results in support.

**Disproportionation Mechanism.** In Scheme 1, we present a proposed mechanism for the photocatalytic reduction of CO<sub>2</sub> by 1 based on the photocatalytic results presented above and additional experiments detailed below. In the photosensitization step, the reduced  $[\text{Ru}(\text{dmb})_3]^{*\bullet+}$  ( $[\text{Ru}(\text{dmb})_3]^{2+/\bullet+} = -1.85 \text{ V vs Fc/Fc+}$ ) transfers an electron to the ligand of Mn complex 1, forming a  $[\text{Mn}(\text{CN})(\text{bpy})(\text{CO})_3]^{*\bullet-}$  species, 2 [eq 1 in Scheme 2;  $[\text{Mn}(\text{CN})(\text{bpy})(\text{CO})_3]^{0/\bullet-} = -1.91 \text{ V vs Fc/Fc+}$ ] [ $[\text{Ru}(\text{dmb})_3]^{2+/\bullet+} = 0.24 \text{ V}$ ;

**Scheme 2. Simplified Description of the Elementary Steps in Photochemical Reduction of CO<sub>2</sub> by 1**



$\text{BNAH}^{0/+} = 0.20 \text{ V vs Fc/Fc}^+$ .<sup>26,29–32</sup> The reduced photosensitizer  $[\text{Ru}(\text{dmb})_3]^{*+}$  is capable of driving catalysis at this potential, but at a diminished rate. Indeed, in comparison to  $\text{MnBr}(\text{bpy})(\text{CO})_3$  much lower rates are observed.<sup>16</sup> Two equivalents of **2** can undergo disproportionation to generate the active  $[\text{Mn}(\text{bpy})(\text{CO})_3]^-$  anion, **3**, and the starting material **1** [Eqn (2) in Scheme 2]. It is presumed that  $\text{HCO}_2\text{H}$  formation in this mechanism results from the protonation of species **3** (by TEOA,  $\text{TEOA}^{*+}$ , or  $\text{TEOA}^+$ ) to generate a Mn hydride, an expected intermediate before  $\text{CO}_2$  insertion, during catalysis.<sup>17,33–37</sup> A preference for  $\text{HCO}_2\text{H}$  is observed in  $N,N$ -DMF-TEOA solution, indicating that the formation of an intermediate hydride species may be favored relative to MeCN.<sup>17</sup> It is also possible for species **3** to form a hydroxycarbonyl species (preferred in MeCN-TEOA) through a direct attack of  $\text{CO}_2$  with subsequent protonation by TEOA or  $\text{TEOA}^+$  (generated by the deprotonation of  $\text{BNAH}^{*+}$ , the expected sacrificial coproduct from photosensitization).<sup>38,39</sup> The resulting  $\eta^1\text{-COOH}$  coordination mode generally yields CO as a product.<sup>40–42</sup> We note another formate formation pathway. It is possible that species **2** may abstract a hydrogen atom from TEOA or  $\text{BNAH}^{*+}$  to generate a hydride species (with presumptive  $\text{CN}^-$  loss) and that the photosensitizer is observed to generate formate in control reactions by an ostensibly analogous mechanism.<sup>43</sup> This presumptive hydride species generated by **2** could also then react with  $\text{CO}_2$  to give  $\text{HCO}_2\text{H}$ . Such reaction pathways are expected to be in competition with the disproportionation mechanism and eventual catalysis by **3**.

The proposed mechanism for the photocatalytic reduction of  $\text{CO}_2$  by  $\text{MnBr}(\text{bpy})(\text{CO})_3$  based on the previous literature<sup>16,17</sup> is also presented for comparison (Scheme 1). In this reaction scheme, the formation of a Mn–Mn bonded dimer is an intermediate step to the formation of a neutral five-coordinate radical species from photoassisted bond cleavage. It is likely at this point in the reaction that the photosensitizer provides the additional electron required to complete the reduction of  $\text{CO}_2$ . The redox potential for  $[\text{Mn}(\text{bpy})(\text{CO})_3]^{*+}$  has not been directly measured, but when using the structural analogue  $\text{MnBr}(6,6'\text{-dimesityl-2,2'-bipyridine})(\text{CO})_3$ , the first reduction observed by cyclic voltammetry becomes a two electron process at  $-1.55 \text{ V vs Fc/Fc}^+$  through the prevention of dimerization, suggesting this can be considered the approximate maximum potential required to generate the anion.<sup>22</sup>

In both the  $N,N$ -DMF-TEOA and MeCN-TEOA solvent systems, the turnover number (TON) for  $\text{HCO}_2\text{H}$ , CO, and  $\text{H}_2$  decreased as the concentration of the Mn complex increased (entries 2, 8, 13, 15, 16, and 18). This observation is consistent with the proposed mechanism of photocatalytic  $\text{CO}_2$  reduction involving an intermediate disproportionation step, *vide infra*.<sup>26</sup> Two equivalents of **1** are required to be reduced by one electron each from  $[\text{Ru}(\text{dmb})_3]^{*+}$  before a disproportionation reaction yields 1 equiv each of the active catalyst  $[\text{Mn}(\text{bpy})-$

$(\text{CO})_3]^-$  and **1**. At high concentrations of **1** and  $[\text{Ru}(\text{dmb})_3]^{*+}$ , mass transport limitations would be expected to affect this process, and limit the overall efficiency. This can be shown in a simplified kinetic description of the overall reaction as shown in Scheme 2 above. Inhibition by increasing concentration of **1** is an expected consequence of the disproportionation reaction in eq 2, if it is assumed to be the rate-limiting step for the formation of **3** and the reaction of **3** with  $\text{CO}_2$  is assumed to be fast relative to  $k_{-2}$ .

This mechanism is further validated by the observation that the TON increases when the ratio of Ru photosensitizer to Mn complex (entries 1, 7, 13, 14, 16 and 17) is increased. The observed increase in catalysis levels off after the ratio of  $[\text{Ru}(\text{dmb})_3]^{*+}$ : **1** reaches 5:1. At this ratio, relative to experiments with equimolar amounts of photosensitizer and catalyst (entries 1–12), there is a 3.6× enhancement in the  $\text{HCO}_2\text{H}$ -TON and 2.3× in the CO-TON in the  $N,N$ -DMF-TEOA system. Likewise, the MeCN-TEOA system shows a 1.8× increase in the  $\text{HCO}_2\text{H}$ -TON and 2.4× in the CO-TON. As shown in eq 1 of Scheme 2, an increased amount of photosensitized Ru ( $\text{Ru}^*$ ) relative to **1** in solution could generate more equivalents of the singly reduced species  $[\text{Mn}(\text{CN})(\text{bpy})(\text{CO})_3]^{*-}$  **2** (Scheme 2). Therefore, more equivalents of the active anion  $[\text{Mn}(\text{bpy})(\text{CO})_3]^-$  **3**, would be formed in eq 2, resulting in an increase in catalyst TONs [eq 3]. After the optimized ratio is reached, the concentration of photosensitizer is no longer a limiting factor and the observed TONs do not change at higher ratios of  $[\text{Ru}(\text{dmb})_3]^{*+}$ : **1**.

Lastly, photodecomposition (mole equiv of CO  $\approx$  2 relative to **1**) in both the MeCN-TEOA and  $N,N$ -DMF-TEOA solvent systems was observed when there was no  $[\text{Ru}(\text{dmb})_3]^{*+}$ ,  $\text{CO}_2$ , or TEOA present (entries 19–31 in Table 2). These experiments also showed that  $[\text{Ru}(\text{dmb})_3]^{*+}$  contributed to  $\text{H}_2$ ,  $\text{HCO}_2\text{H}$ , and CO production, although in a much lower quantity than **1** (entries 20, 24, and 28).<sup>16,17,44</sup>

**Solvent Effects.** The observation that the photocatalytic system is more selective for CO in MeCN-TEOA than in  $N,N$ -DMF-TEOA (which produces more  $\text{HCO}_2\text{H}$ ) suggests the possibility of solvent interactions during the photochemical mechanism. In control reactions with the  $N,N$ -DMF-TEOA solvent system (entries 19–20, 22–25), we note that there is always a small amount of residual  $\text{HCO}_2\text{H}$  which is independent of photocatalysis. The lack of residual  $\text{HCO}_2\text{H}$  in the absence of TEOA (entries 21 and 26) suggests the TEOA is vital for the production of  $\text{HCO}_2\text{H}$  in  $N,N$ -DMF. Furthermore, in the case of entry 22 (a control workup of entry 23 before any irradiation occurred),  $\text{HCO}_2\text{H}$  was detected by  $^1\text{H}$  NMR immediately after mixing the solution in the dark. No  $\text{HCO}_2\text{H}$  was found in the MeCN-TEOA system in analogous experiments. Residual  $\text{HCO}_2\text{H}$  is *only* observed from the interaction between  $N,N$ -DMF and TEOA; this observation is consistent with some recent reports: Vos<sup>27</sup> and Ishida<sup>28</sup> pointed out that  $N,N$ -DMF hydrolyzes spontaneously to give  $\text{HCO}_2\text{H}$  in the presence of water or TEOA. A plot (Figure S1) of  $\text{HCO}_2\text{H}$ -TON vs the concentration of complex **1** shows high linearity for both the 15 and 6 h irradiation times in the  $N,N$ -DMF-TEOA solvent system, suggesting that the amount of  $\text{HCO}_2\text{H}$  formed from  $N,N$ -DMF and TEOA interaction is insignificant under catalytic conditions. Solvent decomposition alone does not explain the large difference in product distribution between the two solvent systems.

To further understand the role of solvent in product selectivity, cyclic voltammetry (CV) was performed both

under Ar and CO<sub>2</sub> saturation. In Figure 1, scans were performed with **1** (1 mM) and tetrabutylammonium

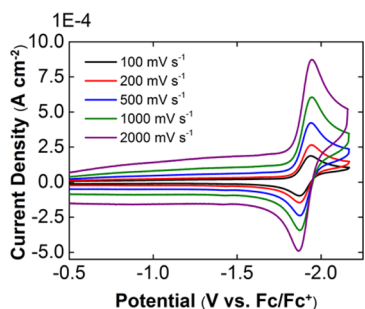


**Figure 1.** Cyclic voltammetry of Mn(CN)(bpy)(CO)<sub>3</sub> **1** under Ar saturation. Conditions: 1 mM **1** in 0.1 TBAPF<sub>6</sub>/N,N-DMF; glassy carbon working electrode, Pt wire counter electrode, Ag/AgCl pseudoreference electrode; referenced to internal Fc standard.

hexafluorophosphate (TBAPF<sub>6</sub>; 0.1 M) as the supporting electrolyte in N,N-DMF under argon (Ar) at scan rates from 100 to 2000 mV/s. The first one-electron, quasireversible redox feature is observed at −1.95 V vs Fc/Fc<sup>+</sup> (*E*<sub>p,c</sub>) with peak-to-peak separation ( $\Delta E_p$ ) of 74 mV. The process is diffusion limited as indicated by the linear relationship between the square root of the scan rate and the peak current (Figure S2). As shown in Figure 2, the addition of TEOA to the solution

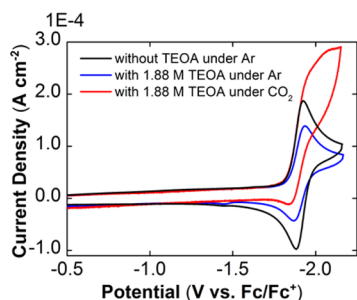


**Figure 2.** Cyclic voltammetry of Mn(CN)(bpy)(CO)<sub>3</sub> **1** under Ar saturation (black), in the presence of TEOA (blue), and under CO<sub>2</sub> saturation (red) in dry N,N-DMF at 100 mV s<sup>−1</sup>. Conditions: 1 mM **1** in 0.1 TBAPF<sub>6</sub>/N,N-DMF; glassy carbon working electrode, Pt wire counter electrode, Ag/AgCl pseudoreference electrode; referenced to internal Fc standard.

under Ar showed a slight current attenuation (0.7×) of the peak current of the first reduction wave (ca. −1.95 V vs Fc/Fc<sup>+</sup>), which is attributed to dilution. When CO<sub>2</sub> is present, the peak current increased to 2.1× that observed under Ar. The current enhancement is consistent with the catalytic reduction of CO<sub>2</sub> by a [Mn(bpy)(CO)<sub>3</sub>]<sup>−</sup> active species.<sup>26</sup>

Interestingly, when TEOA was added to dry MeCN, the redox feature became less reversible and the peak current showed a slight enhancement (2×) under Ar (Figure 3). Such irreversibility is not observed in the absence of TEOA.<sup>26</sup> The presence of CO<sub>2</sub> increased both the irreversibility of the wave and the peak current, suggesting that the interaction of MeCN with TEOA and the reduced species is relevant at this potential, but not for N,N-DMF. This provides important clues for the different product distributions between two solvent systems observed during photocatalysis.

Infrared spectroelectrochemistry (IR-SEC) was used to monitor the microscale electrolysis of complex **1** in the N,N-

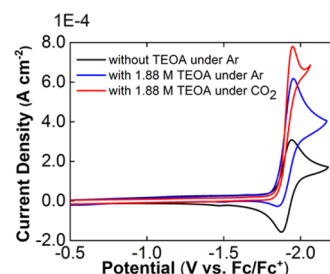


**Figure 3.** Cyclic voltammetry of Mn(CN)(bpy)(CO)<sub>3</sub> **1** under Ar saturation (black), in the presence of TEOA (blue), and under CO<sub>2</sub> saturation (red) in dry MeCN at 100 mV s<sup>−1</sup>. Conditions: 1 mM **1** in 0.1 TBAPF<sub>6</sub>/MeCN; glassy carbon working electrode, Pt wire counter electrode, Ag/AgCl pseudoreference electrode; referenced to internal Fc standard.

DMF-TEOA and MeCN-TEOA solvent systems by IR spectroscopy. IR-SEC allows the starting, intermediate, and product species in solution to be characterized as a function of potential and time.<sup>18,26</sup> When the potential of the IR-SEC cell is shifted stepwise from resting to that of the first reduction in MeCN with added TEOA and **1** (~−1.9 V vs Fc/Fc<sup>+</sup>), two new bands appear at 1911 and 1810 cm<sup>−1</sup> with the concomitant disappearance of the original bands (Figure 4a), which are

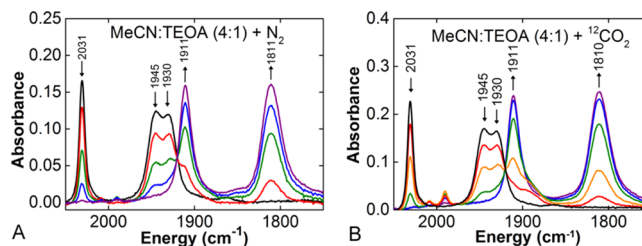


**Figure 4.** Infrared spectra of Mn(CN)(bpy)(CO)<sub>3</sub> (**1**) at controlled potentials (a) in dry MeCN with TEOA under N<sub>2</sub>, and (b) in dry MeCN with TEOA under CO<sub>2</sub>. Conditions: 4 mM **1** in 0.1 TBAPF<sub>6</sub>/MeCN; glassy carbon working electrode, Pt counter electrode, Ag pseudoreference electrode.

assigned to [Mn(bpy)(CO)<sub>3</sub>]<sup>−</sup>. When the MeCN-TEOA solution of **1** is sparged briefly with CO<sub>2</sub> and this experiment is repeated, a band for CO<sub>2</sub> is observed at 2340 cm<sup>−1</sup>. At the potential of the first reduction, this band decreases in intensity, consistent with catalytic consumption of CO<sub>2</sub> (Figure S3). Similar to the case when TEOA is present under N<sub>2</sub> saturation conditions, the only Mn carbonyl bands observed are at 1911 and 1810 cm<sup>−1</sup>, consistent with the formation of the active catalyst species [Mn(bpy)(CO)<sub>3</sub>]<sup>−</sup>.

By comparison, conducting the same experiments in N,N-DMF showed a similar redshift of the Mn carbonyl stretching modes to the active catalyst at the potential of the first reduction, albeit at a slower rate on the experimental time scale (~5 min, Figure 5a). The singly reduced species, [Mn(CN)(bpy)(CO)<sub>3</sub>]<sup>•−</sup>, is more stable under these conditions relative to the results in MeCN. The IR bands visible at resting potential (2026, 1936, and 1927 cm<sup>−1</sup>) almost completely shift to lower frequencies (2003, 1909, and 1893 cm<sup>−1</sup>) when the cell potential is changed from resting to that of the first reduction (~−1.9 V vs Fc/Fc<sup>+</sup>; ~1 min). Previous computations predicted that in MeCN [Mn(CN)(bpy)(CO)<sub>3</sub>]<sup>•−</sup> would have observable IR modes at 2010, 1909, and 1895 cm<sup>−1</sup>; the high frequency mode was experimentally

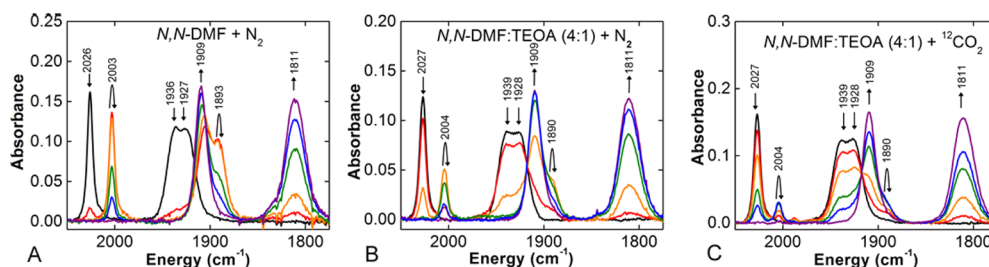


**Figure 5.** Infrared spectra of  $\text{Mn}(\text{CN})(\text{bpy})(\text{CO})_3$  (**1**) at controlled potentials (a) in dry  $N,N$ -DMF under  $\text{N}_2$ , (b) in dry  $N,N$ -DMF with TEOA under  $\text{N}_2$ , and (c) in dry  $N,N$ -DMF with TEOA under  $\text{CO}_2$ . Conditions: 4 mM **1** in 0.1 TBAPF<sub>6</sub>/ $N,N$ -DMF; glassy carbon working electrode, Pt counter electrode, Ag pseudoreference electrode.

observed at  $2007\text{ cm}^{-1}$ .<sup>26</sup> The presence of TEOA and  $\text{CO}_2$  decreases the stability of  $[\text{Mn}(\text{CN})(\text{bpy})(\text{CO})_3]^{*-}$ , as evidenced by a more rapid shift to  $[\text{Mn}(\text{bpy})(\text{CO})_3]^-$  on this time scale ( $1909$  and  $1811\text{ cm}^{-1}$ ;  $\sim 5$  min). In comparison to MeCN-TEOA, however, a more significant amount (as estimated by IR intensity) of the singly reduced species is still observed under these conditions.<sup>17</sup> This difference in the relative stability of  $[\text{Mn}(\text{CN})(\text{bpy})(\text{CO})_3]^{*-}$  in the MeCN- and  $N,N$ -DMF-based solvent systems could explain the observed product selectivities. The higher stability of species **2** observed in  $N,N$ -DMF would allow more time for competing hydrogen atom abstraction pathways involving TEOA or BNAH<sup>•+</sup> to generate  $\text{HCO}_2\text{H}$  via a Mn hydride species.

## CONCLUSION

Using  $[\text{Ru}(\text{dmb})_3]^{2+}$  as a photosensitizer in dry  $N,N$ -DMF-TEOA or MeCN-TEOA solvent mixtures with  $\text{Mn}(\text{CN})(\text{bpy})(\text{CO})_3$  as a catalyst results in photocatalytic  $\text{CO}_2$  reduction through an intermediate disproportionation mechanism. The formation of  $\text{HCO}_2\text{H}$  and CO from  $\text{CO}_2$  decreases with increasing concentration of the Mn complex from 0.1 to 1.0 mM, while the formation of products increases with a higher ratio of  $[\text{Ru}(\text{dmb})_3]^{2+}$ :1. Control reactions have also demonstrated that the  $N,N$ -DMF solvent is not innocent in the formation of  $\text{HCO}_2\text{H}$  in the presence of TEOA. Even in the dark,  $N,N$ -DMF and TEOA generate a measurable amount of  $\text{HCO}_2\text{H}$ . Supplemental CV and IR-SEC studies indicate that although the reduction mechanism in MeCN and  $N,N$ -DMF is similar, there is an observable difference in stability of the  $[\text{Mn}(\text{CN})(\text{bpy})(\text{CO})_3]^{*-}$ . It is clear from these studies that the process of photosensitization by  $[\text{Ru}(\text{dmb})_3]^{2+}$  with BNAH as a sacrificial reductant and the role of TEOA are mechanistically complex and require further investigation to rationally optimize the overall reaction.

## EXPERIMENTAL METHODS

**General.** All reagents were obtained from commercial suppliers and used as received unless otherwise noted. Acetonitrile (MeCN) was obtained from a solvent system under argon (Ar);  $N,N$ -dimethylformamide ( $N,N$ -DMF) and methanol were dried over molecular sieves (3 Å) for 3 days under  $\text{N}_2$  prior to use. Triethanolamine (TEOA) was stored under  $\text{N}_2$ . Tetrabutylammonium hexafluorophosphate (TBAPF<sub>6</sub>) was recrystallized in MeOH twice and dried at  $90\text{ }^\circ\text{C}$  before use.  $\text{Mn}(\text{CN})(\text{bpy})(\text{CO})_3$  was synthesized according to a literature procedure.<sup>26</sup>

<sup>1</sup>H NMR spectra were recorded on a Varian Mercury Plus 400 MHz spectrometer and NMR chemical shifts were referenced to the proton signal of ferrocene. Fourier transform infrared (FTIR) spectra were recorded on a Thermo Nicolet 6700 spectrophotometer running OMNIC software. Absorption spectra were recorded on a CARY

300 Bio UV-Vis spectrophotometer with a quartz cuvette (1 cm path length).

**Photochemical Reactions.** A solution of acetonitrile (MeCN) and triethanolamine (TEOA) ( $\sim 20$  mL; 4:1 v/v) or  $N,N$ -dimethylformamide ( $N,N$ -DMF) and TEOA ( $\sim 20$  mL; 4:1 v/v), which contained  $\text{Mn}(\text{CN})(\text{bpy})(\text{CO})_3$ ,  $[\text{Ru}(\text{dmb})_3]^{2+}$  as a photosensitizer, and 1-benzyl-1,4-dihydroquinoline (BNAH, 0.1 M) as a sacrificial reductant was prepared in a 36 mL quartz cell (NSG Precision Cell, Inc.; path length = 2 cm) sealed with a rubber septum. In the concentration study, solutions containing 0.1, 0.5, and 1.0 mM of both  $\text{Mn}(\text{CN})(\text{bpy})(\text{CO})_3$  and  $[\text{Ru}(\text{dmb})_3]^{2+}$  were prepared and measured. The solution was sparged with dry Ar or  $\text{CO}_2$  gases for 30 min prior to irradiation. The solution was irradiated with a 470 nm LED (ThorLabs, Inc.; bandwidth fwhm = 25 nm) with temperature maintained at  $25.0 \pm 0.1\text{ }^\circ\text{C}$ , and constant stirring throughout the experiment. The light intensity was measured using a NOVA II power meter.

**Product Analysis from Photocatalysis.**<sup>17</sup> The gaseous products,  $\text{H}_2$  and CO, were analyzed by GC-TCD (Hewlett-Packard 7890A Series gas chromatograph) with two molsieve columns ( $30\text{ m} \times 0.53\text{ mm} \times 25\text{ }\mu\text{m}$  film). The 1 mL injection was split between two columns, which use  $\text{N}_2$  and He as carrier gases to measure the quantity of  $\text{H}_2$  and CO, respectively. Turnover numbers (TONs) for the product were calculated as the moles of product divided by the moles of catalyst.

The liquid products were analyzed by a previously reported <sup>1</sup>H NMR (400 MHz Mercury NMR Instrument) method:<sup>10</sup> a known amount of ferrocene (5–8 mg) was added to the irradiated solution in a 5.0 mL volumetric flask to serve as an internal standard, and the solution was sonicated for 10 min. A 1.0 mL syringe was used to transfer a 0.8 mL aliquot of the resulting solution to a 2.0 mL volumetric flask containing 0.1 mmol of Verkade's base (2,8,9-triisopropyl-2,5,8,9-tetraaza-1-phosphabicyclo[3,3,3]undecane).  $\text{CD}_3\text{CN}$  was added to the 2.0 mL mark and the resulting solution was sonicated for another 10 min. The solution was divided into three NMR samples, and each one was run for 128 scans on a Mercury 400 MHz spectrometer at 298 K. The whole workup process was carried out in the dark.

**Cyclic Voltammetry (CV).** CV studies were performed using a BASi Epsilon potentiostat. A 3 mm diameter glassy carbon working electrode (BASi), a platinum (Pt) wire counter electrode, and a silver/silver chloride (Ag/AgCl) wire separated from the bulk solution by a CoralPor tip as a pseudoreference electrode were used in a single compartment cell for all experiments. Experiments were run with and without ferrocene as an internal reference. Electrolyte solutions were composed of dry MeCN or  $N,N$ -DMF, containing 1 mM of catalyst, 0.1 M TBAPF<sub>6</sub> as supporting electrolyte, and with or without 1.88 M TEOA (solvent: TEOA = 4:1 v/v) unless otherwise noted. The electrolyte was purged with Ar or  $\text{CO}_2$  for before cyclic voltammograms were recorded and stirred between successive experiments.

**Infrared Spectroelectrochemistry.** The experimental method, cell design, and setup of the IR-SEC cell have been reported previously.<sup>18</sup> All measurements were made with a Pine Instrument Company model AFCBP1 bipotentiostat. The IR-SEC cell is composed of GC working electrode, Ag pseudoreference electrode,

and Pt counter electrode. All potentials were referenced to the pseudoreference Ag/Ag<sup>+</sup>, ~+200 mV higher than the Fc/Fc<sup>+</sup> couple. The solution containing 4 mM Mn complex and 0.1 M TBAPF<sub>6</sub> in dry MeCN or N,N-DMF with or without TEOA (solvent: TEOA = 4:1 v/v) was sparged with N<sub>2</sub> or CO<sub>2</sub> and then injected into the IR-SEC cell to form a thin liquid layer for bulk electrolysis. The potential was changed stepwise and the solution was monitored with Fourier transform reflectance IR off the electrode surface over time.

**Preparation of Ru(dmb)<sub>3</sub>(PF<sub>6</sub>)<sub>2</sub>.** The photosensitizer, Ru(dmb)<sub>3</sub>(PF<sub>6</sub>)<sub>2</sub> (dmb = 4,4'-dimethyl-2,2'-bipyridine) was synthesized from RuCl<sub>3</sub>·xH<sub>2</sub>O (91.7 mg, 0.169 mmol) and dmb (46.5 mg, 0.255 mmol) according to literature<sup>45</sup> and further purified by recrystallization with acetone-diethyl ether. All characterization was consistent with previous reports; yield: 55.2 mg (34.6%).

## ■ ASSOCIATED CONTENT

### 🔗 Supporting Information

The Supporting Information is available free of charge on the ACS Publications website at DOI: 10.1021/acs.inorgchem.6b00379.

NMR, FTIR, and UV–vis spectra data (PDF)

## ■ AUTHOR INFORMATION

### Corresponding Author

\*E-mail: ckubiak@ucsd.edu (C.P.K.).

### Notes

The authors declare no competing financial interest.

## ■ ACKNOWLEDGMENTS

P.L.C., C.W.M., and C.P.K. acknowledge support for this work from the AFOSR through a Basic Research Initiative (BRI) Grant (No. FA9550-12-1-0414). J.A. acknowledges support from the NSF (CHE-1361178).

## ■ REFERENCES

- (1) Lewis, N. S.; Nocera, D. G. *Proc. Natl. Acad. Sci. U. S. A.* **2006**, *103*, 15729.
- (2) Balzani, V.; Credi, A.; Venturi, M. *ChemSusChem* **2008**, *1*, 26.
- (3) Benson, E. E.; Kubiak, C. P.; Sathrum, A. J.; Smieja, J. M. *Chem. Soc. Rev.* **2009**, *38*, 89.
- (4) Ishida, H.; Terada, T.; Tanaka, K.; Tanaka, T. *Inorg. Chem.* **1990**, *29*, 905.
- (5) Lehn, J. M.; Ziessel, R. *J. Organomet. Chem.* **1990**, *382*, 157.
- (6) Kumar, B.; Smieja, J. M.; Kubiak, C. P. *J. Phys. Chem. C* **2010**, *114*, 14220.
- (7) Tamaki, Y.; Morimoto, T.; Koike, K.; Ishitani, O. *Proc. Natl. Acad. Sci. U. S. A.* **2012**, *109*, 15673.
- (8) Morimoto, T.; Nakajima, T.; Sawa, S.; Nakanishi, R.; Imori, D.; Ishitani, O. *J. Am. Chem. Soc.* **2013**, *135*, 16825.
- (9) Shakeri, J.; Farrokhpour, H.; Hadadzadeh, H.; Joshaghani, M. *RSC Adv.* **2015**, *5*, 41125.
- (10) Smieja, J. M.; Sampson, M. D.; Grice, K. A.; Benson, E. E.; Froehlich, J. D.; Kubiak, C. P. *Inorg. Chem.* **2013**, *52*, 2484.
- (11) In *CRC Handbook of Chemistry and Physics*, 92nd ed.; Haynes, W. M., Ed.; CRC Press: Boca Raton: FL, 2011; p 2011.
- (12) Juris, A.; Balzani, V.; Barigelli, F.; Campagna, S.; Belser, P.; von Zelewsky, A. *Coord. Chem. Rev.* **1988**, *84*, 85.
- (13) Matsuoka, S.; Yamamoto, K.; Ogata, T.; Kusaba, M.; Nakashima, N.; Fujita, E.; Yanagida, S. *J. Am. Chem. Soc.* **1993**, *115*, 601.
- (14) Loudet, A.; Burgess, K. *Chem. Rev.* **2007**, *107*, 4891.
- (15) Bourrez, M.; Molton, F.; Chardon-Noblat, S.; Deronzier, A. *Angew. Chem., Int. Ed.* **2011**, *50*, 9903.
- (16) Takeda, H.; Koizumi, H.; Okamoto, K.; Ishitani, O. *Chem. Commun.* **2014**, *50*, 1491.

(17) Fei, H. H.; Sampson, M. D.; Lee, Y.; Kubiak, C. P.; Cohen, S. M. *Inorg. Chem.* **2015**, *54*, 6821.

(18) Machan, C. W.; Sampson, M. D.; Chabolla, S. A.; Dang, T.; Kubiak, C. P. *Organometallics* **2014**, *33*, 4550.

(19) Grills, D. C.; Farrington, J. A.; Layne, B. H.; Lymar, S. V.; Mello, B. A.; Preses, J. M.; Wishart, J. F. *J. Am. Chem. Soc.* **2014**, *136*, 5563.

(20) Riplinger, C.; Sampson, M. D.; Ritzmann, A. M.; Kubiak, C. P.; Carter, E. A. *J. Am. Chem. Soc.* **2014**, *136*, 16285.

(21) Riplinger, C.; Carter, E. A. *ACS Catal.* **2015**, *5*, 900.

(22) Sampson, M. D.; Nguyen, A. D.; Grice, K. A.; Moore, C. E.; Rheingold, A. L.; Kubiak, C. P. *J. Am. Chem. Soc.* **2014**, *136*, 5460.

(23) Meyer, T. J.; Caspar, J. V. *Chem. Rev.* **1985**, *85*, 187.

(24) Allen, D. M.; Cox, A.; Kemp, T. J.; Sultana, Q.; Pitts, R. B. *J. Chem. Soc., Dalton Trans.* **1976**, 1189.

(25) Van der Graaf, T.; Hofstra, R. M. J.; Schilder, P. G. M.; Rijkhoff, M.; Stufkens, D. J.; Vanderlinden, J. G. M. *Organometallics* **1991**, *10*, 3668.

(26) Machan, C. W.; Stanton, C. J.; Vandezande, J. E.; Majetich, G. F.; Schaefer, H. F.; Kubiak, C. P.; Agarwal, J. *Inorg. Chem.* **2015**, *54*, 8849.

(27) Paul, A.; Connolly, D.; Schulz, M.; Pryce, M. T.; Vos, J. G. *Inorg. Chem.* **2012**, *51*, 1977.

(28) Kuramochi, Y.; Kamiya, M.; Ishida, H. *Inorg. Chem.* **2014**, *53*, 3326.

(29) Kitamura, N.; Rajagopal, S.; Tazuke, S. *J. Phys. Chem.* **1987**, *91*, 3767.

(30) Connelly, N. G.; Geiger, W. E. *Chem. Rev.* **1996**, *96*, 877.

(31) Ross, H. B.; Boldaji, M.; Rillema, D. P.; Blanton, C. B.; White, R. P. *Inorg. Chem.* **1989**, *28*, 1013.

(32) Fukuzumi, S.; Hironaka, K.; Nishizawa, N.; Tanaka, T. *Bull. Chem. Soc. Jpn.* **1983**, *56*, 2220.

(33) Sullivan, B. P.; Meyer, T. J. *Organometallics* **1986**, *5*, 1500.

(34) Agarwal, J.; Johnson, R. P.; Li, G. H. *J. Phys. Chem. A* **2011**, *115*, 2877.

(35) Chan, S. F.; Chou, M.; Creutz, C.; Matsubara, T.; Sutin, N. *J. Am. Chem. Soc.* **1981**, *103*, 369.

(36) Koike, K.; Hori, H.; Ishizuka, M.; Westwell, J. R.; Takeuchi, K.; Ibusuki, T.; Enjouji, K.; Konno, H.; Sakamoto, K.; Ishitani, O. *Organometallics* **1997**, *16*, 5724.

(37) Franco, F.; Cometto, C.; Ferrero Vallana, F.; Sordello, F.; Priola, E.; Minero, C.; Nervi, C.; Gobetto, R. *Chem. Commun.* **2014**, *50*, 14670.

(38) Tamaki, Y.; Watanabe, K.; Koike, K.; Inoue, H.; Morimoto, T.; Ishitani, O. *Faraday Discuss.* **2012**, *155*, 115.

(39) Gholamkhash, B.; Mametsuka, H.; Koike, K.; Tanabe, T.; Furue, M.; Ishitani, O. *Inorg. Chem.* **2005**, *44*, 2326.

(40) Keith, J. A.; Grice, K. A.; Kubiak, C. P.; Carter, E. A. *J. Am. Chem. Soc.* **2013**, *135*, 15823.

(41) Agarwal, J.; Shaw, T. W.; Schaefer, H. F.; Bocarsly, A. B. *Inorg. Chem.* **2015**, *54*, 5285.

(42) Keene, F. R.; Sullivan, B. P. In *Electrochemical and Electrocatalytic Reactions of Carbon Dioxide*; Sullivan, B. P., Krist, K., Guard, H. E., Ed.; Elsevier: Amsterdam, 1993; p 118.

(43) Gerasimov, O. V.; Parmon, V. N. *Russ. Chem. Rev.* **1992**, *61*, 154.

(44) Priyadarshani, N.; Liang, Y. N.; Suriboot, J.; Bazzi, H. S.; Bergbreiter, D. E. *ACS Macro Lett.* **2013**, *2*, 571.

(45) Hawecker, J.; Lehn, J. M.; Ziessel, R. *J. Chem. Soc., Chem. Commun.* **1985**, 56.